C. P. No. 620

C. P. No. 620

MINISTRY OF AVIATION

AERONAUTICAL RESEARCH COUNCIL

CURRENT PAPERS

The Construction and Testing of a Large Axial Flow Compressor

By

R. Shaw and A. Lewkowicz

LONDON: HER MAJESTY'S STATIONERY OFFICE

1963

Price 2s 6d Net

C.P. NO.620

The Construction and Testing of a Large Axial Flow Compressor

- By -
R. Shaw and A. Lewkowicz

Communicated by Prof. J. H. Horlock

May, 1962

SUMMARY

The construction of a large low speed research compressor is described, together with some preliminary performance tests of a single stage arrangement at various speeds. The stalled region was investigated at all speeds, but at one speed a fuller investigation under stalled condition was carried out. At the low speeds involved an indication of stall cell frequency could be ascertained by observation of the static pressure manometer fluctuations.

1. Description of the Rig

A large low speed compressor has been built at the University of Liverpool to investigate the effect of the radial movement of the blade surface boundary layer on blade section performance. The compressor, the air intake duct made in fibreglass reinforced Polyester resin, and the method of pressure transmission from the moving blades are described.

1.1 Compressor

The complete unit is shown in Figs. 1 and 2. The rotor, which is 3 ft in diameter, and the stator, which has an inside diameter of 4 ft, are fabricated in mild steel. The blades have a constant section (10 C4/30 C50), a chord of 3 in. pitch/chord ratio of 1, and are set to a stagger angle of 36°. These blades are aluminium alloy forgings and are provided with simple cylindrical root platforms and threaded root fixings to permit variation in the stagger angle. To facilitate manufacture one set of forging dies was used for all blades, but all blades were provided initially with a root fixing at each end. One root fixing was used for rotor and stator blades whilst the other was used for the inlet guide vanes, which operate at +5.7° incidence as a result of this manufacturing simplification.

The design speed of the compressor is 684 rev/min and the design mass flow rate is 31.6 lb_m/sec, giving 50% reaction at the blade tip.

The rotor is located between bearings and since this involves separate support pedestals, both these ball bearings (parts 22 and 23) are self aligning. One of these bearings also takes the end thrust and locates the rotor. The drive shaft (part 8) with its own two bearings (parts 4)

is/

Replaces A.R.C.23,817

is connected to the rotor shaft by means of a flexible coupling (part 9). The drive is obtained from a d.c. motor (part 24) via V-ropes which pass through the diffuser. The diffuser has an inner cone made in timber and plywood whilst the octagonal outer wall is made in timber and Masonite board. The throttle (part 21) consists of 20 gauge sheet steel covering a frame of mild steel rods.

1.2 Air intake duct

Since it was considered desirable to eliminate all possible upstream disturbances the form of air intake shown in Fig. 1 was chosen in preference to a straight axial entry which would have necessitated radial supports for the inner wall. The air intake profiles are based on a modified two-dimensional potential flow analysis and the resultant three-dimensional form presented obvious manufacturing difficulties. To obtain the accuracy required, a metal intake would have been too costly and too heavy. A construction using thin wooden plankings attached to wood formers would also have been costly and heavy and there would have been some uncertainty about the stability of the wooden formers. It was therefore decided to use fibreglass reinforced Polyester resin for this intake. A general purpose flexible lay-up resin with thixotropic ingredient and accelerator was used in conjunction with fibreglass chopped strand mat and surfacing mat.

This method of manufacture therefore necessitated the construction of two accurate axisymmetric moulds, similar to those used in foundry loam moulding. Fig. 3 shows the assembly of the bottom plate and radial grounds of the mould for the inner wall together with the centre spindle and strickle board. A distance of about 3/4 in. was left between the profiled edge of the strickle board and the grounds to allow for the build-up of the mould. A layer of expanded metal was placed over the grounds and this was then covered with a layer of sand and cement about $\frac{1}{2}$ in. thick. Finally a layer of board plaster, 3/16 in. thick, was slurried on, whilst the strickle was continuously rotated. The completed mould and strickle board for the outer wall is shown in Fig. 4. The finished moulds were then left for three weeks to dry. They were then sealed, painted, wax-polished and finally coated with Polyvinyl Alcohol parting agent.

Next the fibreglass chopped strand mat and surfacing mat were cut into sufficient segments to provide two layers of each. The segments themselves were slit as required to ensure overlapping of the mat rather than wrinkling at the points of greatest curvature. The polyester resin was then mixed with the correct amount of accelerator and catalyst hardner in quantities up to 12 lb, which was the maximum amount usable before gelling occurred. A coat of resin was applied to the mould and then a layer of surface mat was added and stippled into the resin. Another coat of resin was applied, followed by the first layer of chopped mat, which was carefully stippled and rolled into the resin to remove all air bubbles. One more layer of chopped mat and one of surfacing mat were then applied between coatings of resin, and the mould was then left to gell and age-harden for about 8 or 9 days.

The fibreglass was released from the mould by tapping and lifting from the edge inwards. The mould was then marked with centre lines and these were traced onto the fibreglass after reinsertion in the mould. Radial strengthening ribs were then made from fibreglass and resin placed over cardboard formers. Metal brackets for attachments, wood blocks for pressure tappings and a flange were also added. Since a good surface finish was obtained from the mould it was then only necessary to polish the important surfaces very lightly.

1.3/

1.3 Instrumentation

Instrumentation was provided to record the following information at 5 equally spaced circumferential positions:-

(a) Intake static pressure (inner and outer ducts).

(b) Intake total pressure (traverse).

(c) Compressor inlet static pressure (inner and outer wall).

(d) Compressor outlet static pressure (inner and outer wall).

An ammeter and voltmeter were connected into the armature circuit of the d.c. motor for measurement of the input power. The speed was ascertained by revolution counter.

Since the tests described in this paper, the compressor has been modified to permit pitot-static-yawmeter traverse behind each blade row. Full radial traverse and circumferential traverse over two blade pitches is allowed by circumferential slots cut in stator (5/8 in. wide x 8 in. long). Sealing of the slots is achieved by means of sliding flexible brass strips which are constrained in such a way as to remain flush with the inside wall of the stator. A small rectangular opening has also been cut in the stator to allow for the "painting" of blades for flow visualisation experiments. Support brackets for hot wire anemometers have also been provided.

In order to record the surface static pressures on the rotor blade, direct pressure transmission will be employed in preference to using pressure transducers and electrical transmission. The method employed is illustrated in Fig. 5 which shows a half-sectioned elevation of the pressure transmission unit. Static pressure tapping connections from the moving blades will pass through the rotor rim and down the central web of the rotor to which they will be secured. At the rotor hub these connections will pass through the flange and along the bore of the hollow rotor stub shaft, and into the bore of the hollow pressure transmission unit shaft (part 1, Fig. 5). One such connection, as shown, passes along the bore and is bent to pass through the wall of the shaft to which it is soldered. There are 18 connections, each communicating with an annular space formed by the hollow shaft (part 1), the housing (part 6) and pairs of rubber ring oil seals (parts 4). Holes drilled through the housing permit the transmission of the pressures from these annular spaces to a multi-tube manometer. Corrections will be applied to these measured pressures to allow for the radial pressure gradients set up in the revolving radial sections of the connection tubing.

2. Initial Testing Difficulties

Although the rotor has been carefully balanced on a vibrating reed type of balancing machine, made specifically for this purpose, initial running indicated the presence of a resonant torsional oscillation of the inlet end support pedestal. Stiffening of this pedestal reduced the vibration to an acceptable amplitude, but as a safety precaution, microswitches have been fitted to a beam, which is fixed to the stator, in such a way that they are almost in contact with the rotor stub shaft. The switches are connected to a relay and cut-out so that the compressor is automatically shut down if excessive vibration occurs.

Although the compressor had been designed to achieve perfect axisymmetric flow, the initial performance readings indicated a transverse asymmetry, due to the proximity of the laboratory wall. This was cured by building a partition on the other side of the compressor to ensure equal return airflow paths. Even then some asymmetry still existed and this was found to be due to the support struts of the downstream pedestal (part 3, Fig. 1). To reduce the interference of these struts by means of

aerofoil sections was not practicable, so further dummy struts were placed equally spaced around the annulus. These had the desired effect and the flow is now nearly axisymmetric.

3. Test Procedure and Calculation of Results

The pulley reduction ratio was first ascertained by simultaneously recording compressor and motor shaft speeds. The intake was then traversed at the 5 circumferential positions and at 2 different speeds, and the mean intake velocity thus calibrated against the intake wall static pressure (see Appendix).

A series of 9 tests was then carried out starting at 116 r.p.m. compressor speed and increasing to 650 r.p.m. At each speed the throttle opening was set initially to 16 in. (corresponding to a flow coefficient $\phi = 0.65$) and was closed progressively to the stall point (throttle opening = $2\frac{1}{2}$ in., $\phi = 0.42$), considerable care being taken to obtain readings at the points just prior to stall, and immediately after stall. A sudden transition occurred at the onset of stall with a marked fall in the static pressure rise across the compressor. It proved quite impossible to operate the compressor at an intermediate point. The stall onset lines are therefore shown dotted on the graph (Fig. 6). Several further results were then obtained down to $\phi = 0.2$ (which was the condition at the original limit of throttle closure). Rotating stall was detected audibly and also by observation of oscillations of the fluid in the manometer tubes connected to the 5 circumferential static pressure positions. The fluid was seen quite clearly to be raised in each tube in turn at a frequency between approximately 1 and 3 cycles per second.

At all speeds except the lowest the throttle was then opened progressively from the positions for stalled operation through to unstalled operation. From the throttle positions during the unstalling it was apparent that the behaviour on throttle opening was different from that for throttle closing, so that as many points as possible were obtained in this region.

In order to obtain results to zero flow ($\phi = 0$) the octagonal diffuser exit was provided with baffles to cover the corners and present a circular form to the throttle cone. At 422 r.p.m. further results were obtained down to $\phi = 0$ and a further transition noted at $\phi = 0.1$ when both the audible and visual indications of rotating stall ceased. On opening the throttle a difference of behaviour between the throttle opening and closing cases were also observed in this region.

On completion of the compressor tests the unit was opened up and a Prony brake installed in place of the rotor. The electrical power and corresponding brake power were then observed for the range of speeds and loads employed in the compressor tests. Hence the mechanical and electrical losses were computed and a small correction applied for the different disc friction losses of the rotor and brake. Compressor input power and hence stagnation temperature rise coefficient $[C_p\Delta T_o/\frac{1}{2}U_m^2]$ were then computed. An efficiency $\eta = \left[\frac{\Delta p}{\frac{1}{2}\rho U_m^2}\right] \Big/ \left[\frac{C_p \Delta T_o}{\frac{1}{2}U_m^2}\right]$ was then obtained and plotted against ϕ. At η_{max} the static pressure rise coefficient was converted to the stagnation pressure rise coefficient $[\Delta p_o/\frac{1}{2}\rho U_m^2]$ and the "total-to-total" efficiency η_{tt} calculated. For the purpose of computing the exit dynamic pressure the air angle at exit from the stator blade was estimated from data by Howell[2].

4./

4. Discussion of Results

Since the power calibration was found to be unreliable, especially at the lower speeds it was not possible to accurately determine the efficiency. The results however indicated a maximum "total-to-total" efficiency of approximately 85% at a Reynolds number of 1.985×10^5. It was not possible to compare the effects of Reynolds number on efficiency with Carter's prediction[1] because of this uncertainty in the power measurement.

The static pressure rise coefficient ψ/flow coefficient ϕ characteristic for the Reynolds number range 0.337×10^5 to 1.895×10^5 is plotted in Fig. 6 and shows no Reynolds number effect; the characteristic for each speed being represented by the same curve, except for small random variations of ϕ at the pre-stall point (ϕ = 0.41 to 0.435; ψ = 0.65). At this point further reduction of the flow coefficient caused a sudden fall in the static pressure rise coefficient to the first stall point. (ϕ= 0.35 to 0.365; ψ = 0.46). It seems probable that this sudden change was due only to the onset of stall, although it is possible that the inability to operate at any intermediate point in this region could be due to a correspondence of the compressor and throttle operating lines.

The numbers beside the points on the performance curve (Fig. 6) indicate the rotating stall frequency in cycles per minute and show values ranging from 1/7th to 1/2 the compressor rotational speed. Since it was not possible to determine the number of stall cells, the speed of any particular stall cell cannot be determined from these preliminary tests.

On opening the throttle from the stalled region, the different behaviour indicated by new throttle settings and also by the changing rotating stall frequency is confirmed by Fig. 6 where a small but distinct "hysteresis loop" is seen on the characteristic. It was not only possible to operate at values of flow coefficient greater than that for the first stall point for closure of the throttle, but in most cases any intermediate point up to the unstalled part of the characteristic could be found. In this region however the rotating stall frequency is seen to be higher. The size and form of the hysteresis loop is seen to be much the same for all Reynolds numbers.

At 422 r.p.m., closure of the throttle towards the condition $\phi = 0$ was marked by a further, but smaller, sudden change at about $\phi = 0.1$, when both the audible and visible indication of a rotating stall ceased, presumably indicating the onset of complete circumferential stall. On reopening the throttle a small second "hysteresis loop" was found as shown in Fig. 6, indicating a delay in the breakdown of the complete stall into rotating stall. Furthermore, on re-entering the rotating stall region (ϕ increasing) the frequency of rotating stall was found to be much higher (208) compared with the frequency (64) when leaving the rotating stall region (ϕ decreasing).

The comparison of the actual characteristic with that obtained by the Howell method[2] shows that the Howell prediction is a little too optimistic in this case, but the two characteristics have the same general shape, typical of a low speed compressor.

5. Conclusions

Two "hysteresis loops" exist in the static pressure rise coefficient/flow coefficient characteristic. One occurs at a low flow coefficient, due to the delayed transition from complete stall to rotating stall as the flow is increased. The second occurs at a higher flow coefficient, due to the delayed transition from rotating stall to the unstalled condition as the flow is increased.

The/

The static pressure rise coefficient/flow coefficient characteristic is unaffected by Reynolds number in the Reynolds number range 0.337×10^5 to 1.985×10^5.

6. Acknowledgments

The excellent workmanship of many members of the Departmental Workshops is acknowledged. In particular Mr. H. Ainsworth and his staff of the Wood Workshop are thanked for so successfully making the fibreglass air intake and other ducting and Mr. J. Cowie and Mr. C. Rigby of the Metal Workshop for the detailed work on the compressor itself.

The help given by the English Electric Co. with the manufacture of the rotor and stator and Bristol Siddeley Engines with the manufacture of the blading is also gratefully acknowledged.

We also thank Prof. Horlock for his help and guidance with this work and the Ministry of Aviation who have sponsored the building of this compressor.

Notation

c_x = axial velocity

U_m = mean blade velocity

$\phi = \dfrac{c_x}{U_m}$ = flow coefficient

Δp = static pressure rise across the stage (including IGV's)

ρ = density

$\psi = \dfrac{\Delta p}{\frac{1}{2}\rho U_m^2}$ = static pressure rise coefficient

$\dfrac{C_p \Delta T_o}{\frac{1}{2}U_m^2}$ = stagnation temperature rise coefficient

$\dfrac{\Delta p_o}{\frac{1}{2}\rho U_m^2}$ = stagnation pressure rise coefficient

$\eta = \left[\dfrac{\Delta p}{\frac{1}{2}\rho U_m^2}\right] \Big/ \left[\dfrac{C_p \Delta T_o}{\frac{1}{2}U_m^2}\right]$

$\eta_{tt} = \left[\dfrac{\Delta p_o}{\frac{1}{2}\rho U_m^2}\right] \Big/ \left[\dfrac{C_p \Delta T_o}{\frac{1}{2}U_m^2}\right]$ = "total-to-total" efficiency

C_m = mean intake velocity

p_a = atmospheric pressure

p = mean static pressure at the intake duct

References/

References

No.	Author(s)	Title, etc.
1	A. D. S. Carter, C. E. Moss, G. R. Green and G. G. Annear	The effect of Reynolds number on the performance of a single stage compressor. A.R.C. R. & M. No.3184, May, 1957.
2	A. R. Howell	Fluid dynamics of axial compressors. Proc. I. Mech. E. No.153, 1945.

APPENDIX/

APPENDIX

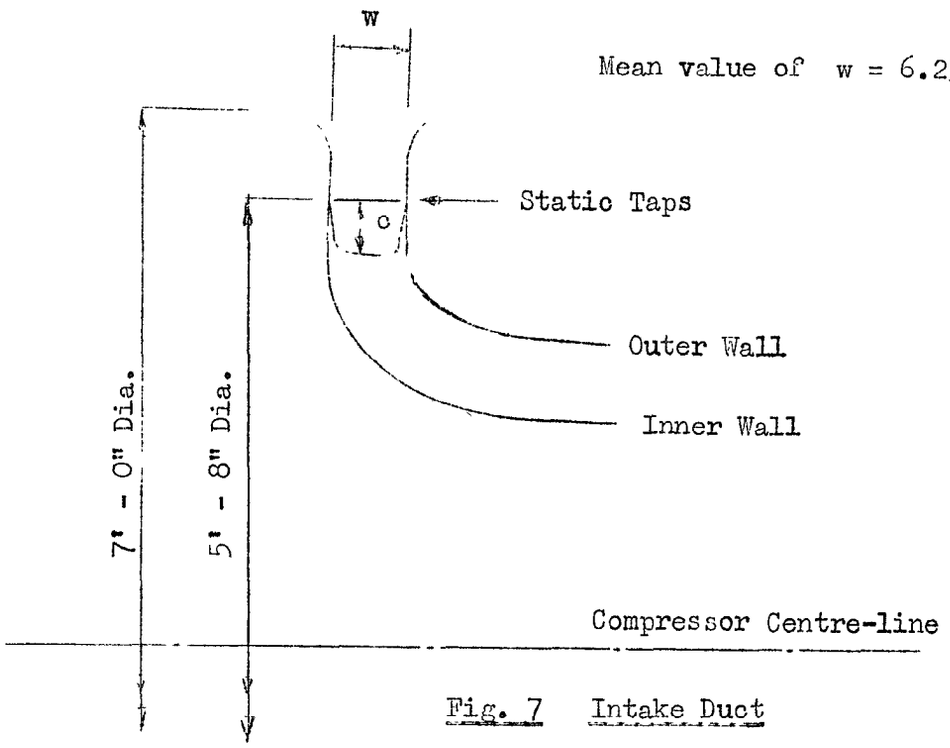

Fig. 7 Intake Duct

The sketch shows the significant dimensions of the intake duct. The total pressure was measured across the intake and together with the wall static pressures was used to calculate the intake velocity distribution. Due to the curvature of the streamlines the static pressure was found to be slightly greater on the inner wall so that the velocity increased slightly towards the outer wall of the duct giving the velocity distribution shown in the sketch. The boundary layer was not fully developed, being only approximately 1/10th in. thick. By graphical methods the mean intake velocity $c_m = \int \frac{c\,dw}{w}$ was determined. For the various circumferential positions and speeds the velocity coefficient

$$\left[\frac{c_m}{\sqrt{\frac{p_a - p}{\frac{1}{2}\rho}}}\right]$$

was found to vary only slightly and a mean value of 0.985 was therefore used in the calculations.

WS

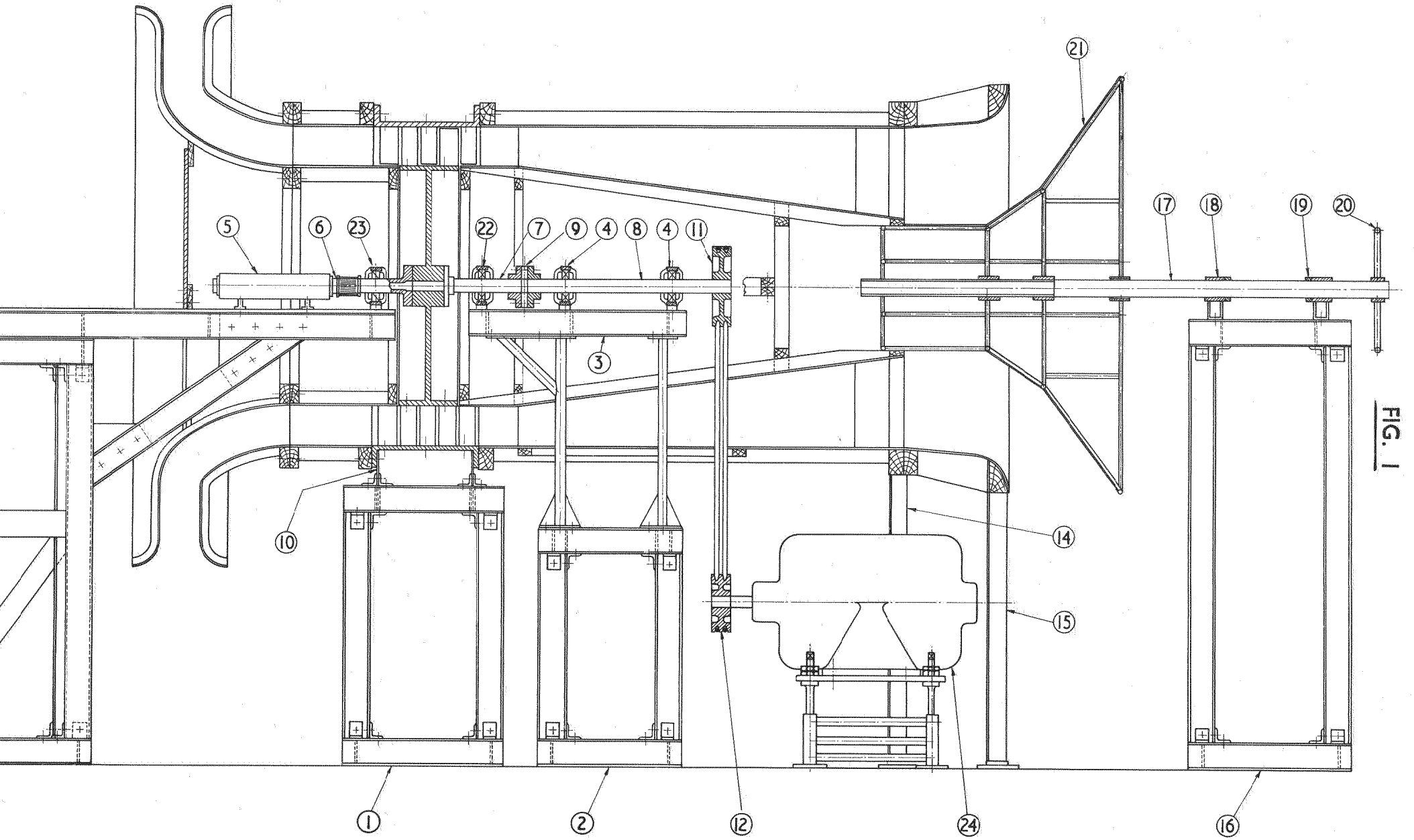

FIG. 1

General arrangement of research compressor

FIG. 2.

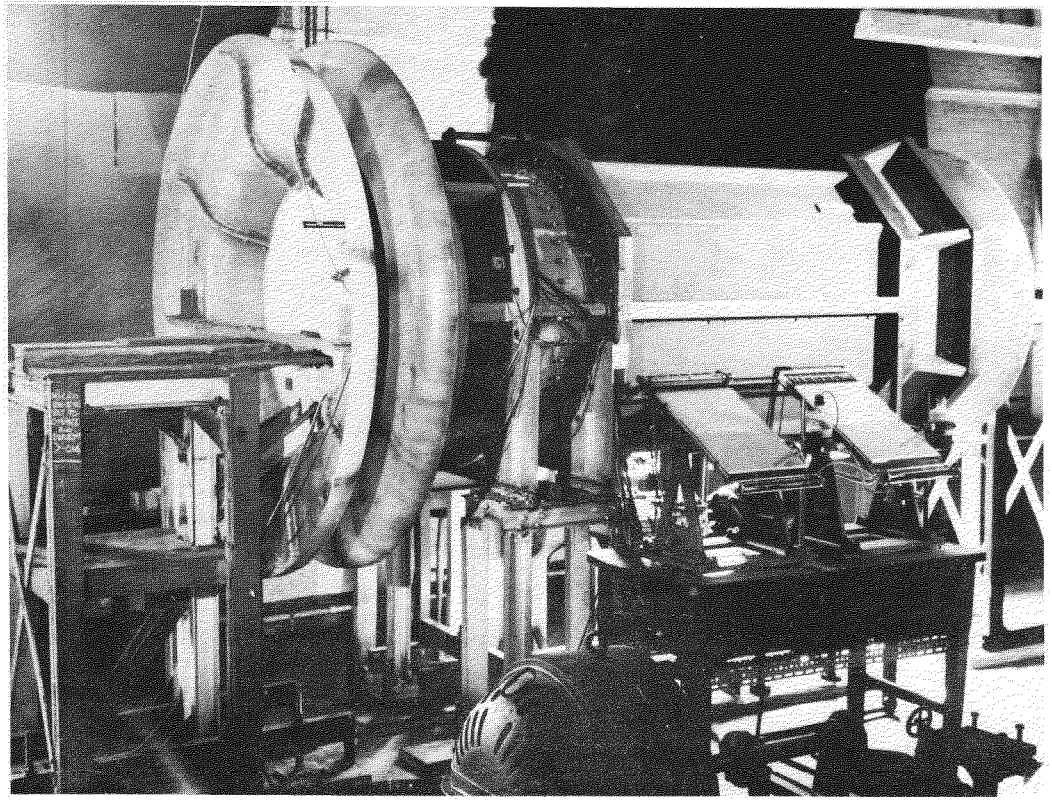

Fig. 2. Research compressor

FIGS. 3 & 4.

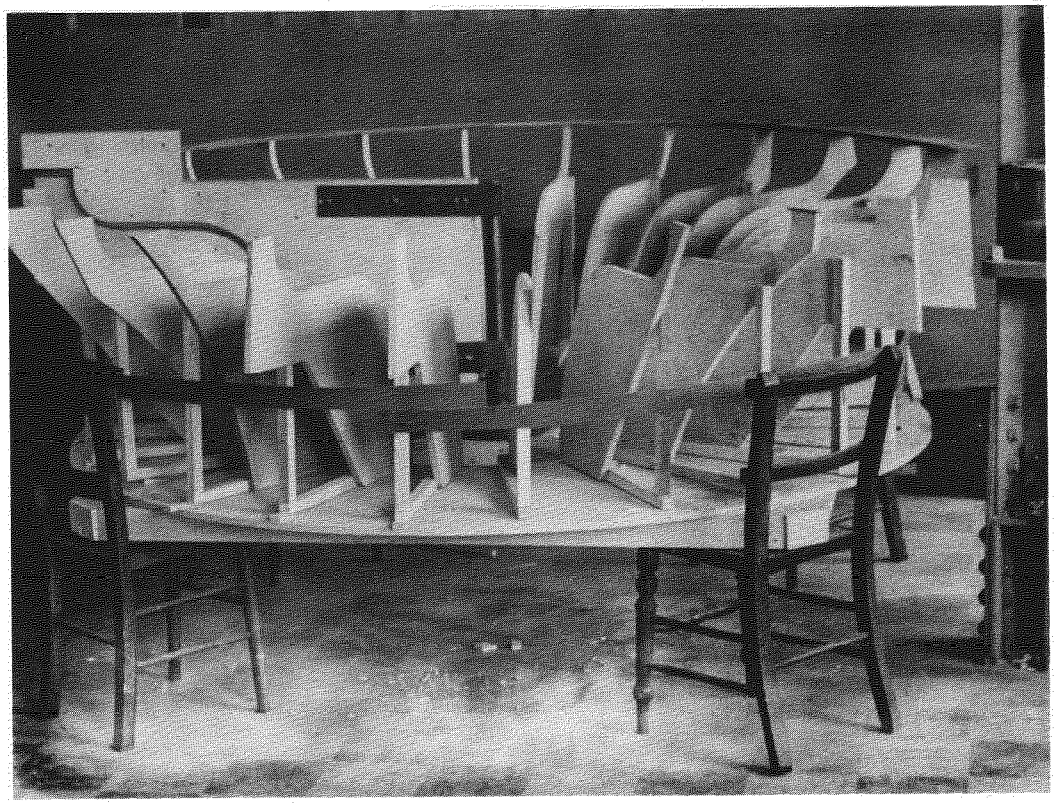

Fig. 3. Assembly of mould for inner wall of air intake duct.

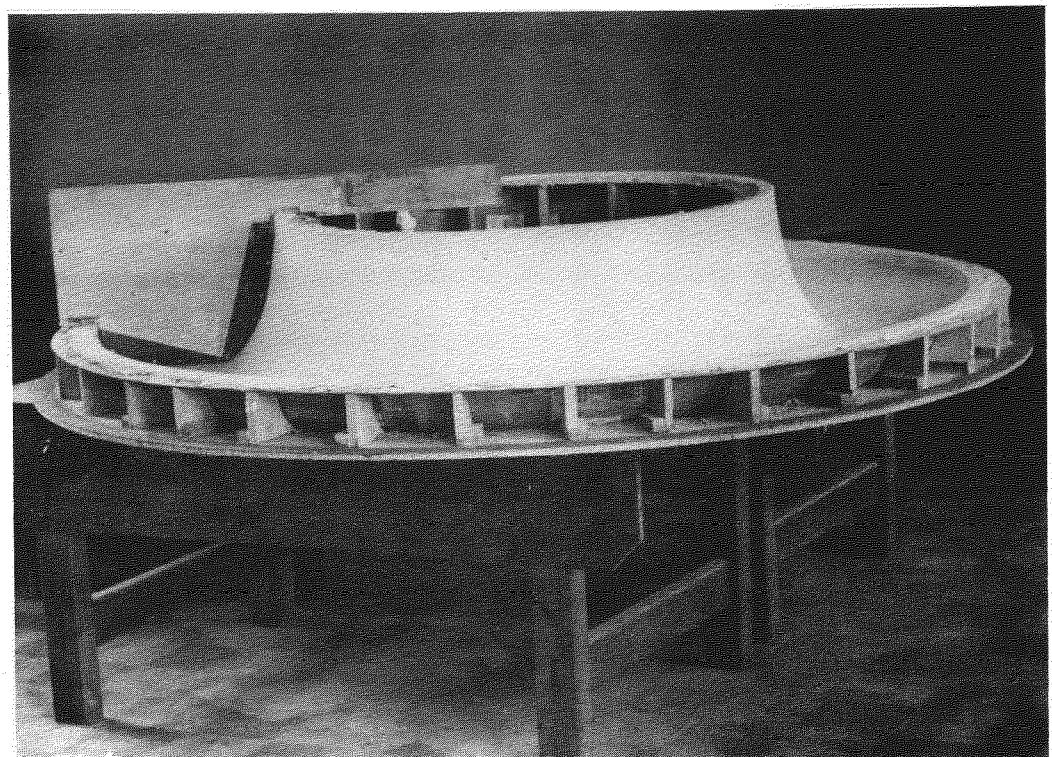

FIG. 5

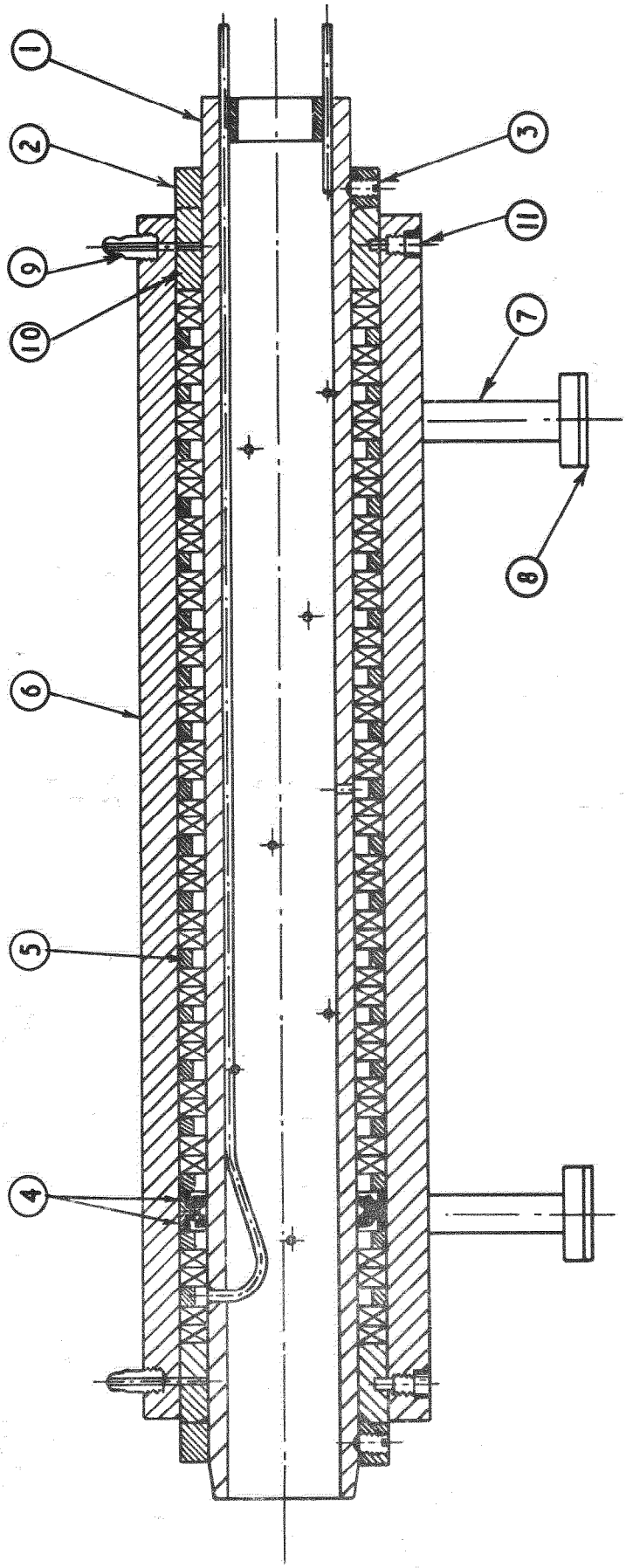

Pressure transmission unit

FIG. 6

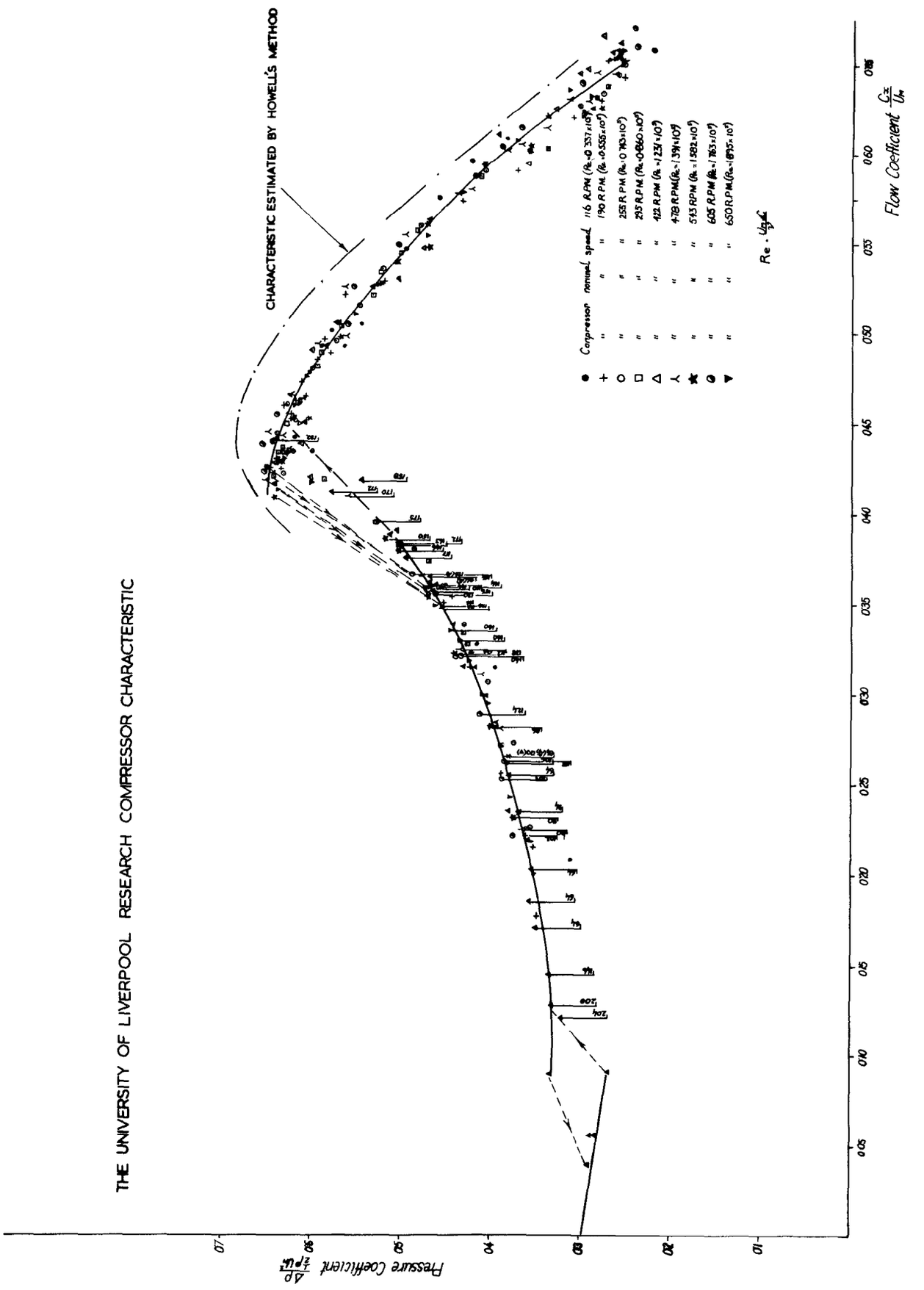
THE UNIVERSITY OF LIVERPOOL RESEARCH COMPRESSOR CHARACTERISTIC
CHARACTERISTIC ESTIMATED BY HOWELL'S METHOD
Compressor nominal speed 116 R.P.M (Re.=0.337×10⁵)
" " 190 R.P.M. (Re.=0.555×10⁵)
" " 253 R.P.M (Re.=0.743×10⁵)
" " 295 R.P.M (Re.=0.860×10⁵)
" " 412 R.P.M (Re.=1.23×10⁵)
" " 478 R.P.M (Re.=1.39×10⁵)
" " 543 R.P.M (Re.=1.582×10⁵)
" " 605 R.P.M (Re.=1.765×10⁵)
" " 650 R.P.M (Re.=1.875×10⁵)
Re. Upstream
Pressure Coefficient $\frac{\Delta P}{\frac{1}{2}\rho U_x^2}$
Flow Coefficient $\frac{C_x}{U_m}$

A.R.C. C.P. No.620 May 1962

Shaw, R. and Lewkowicz, A.

THE CONSTRUCTION AND TESTING OF A LARGE AXIAL FLOW COMPRESSOR

The construction of a large low speed research compressor is described, together with some preliminary performance tests of a single stage arrangement at various speeds. The stalled region was investigated at all speeds, but at one speed a fuller investigation under stalled condition was carried out. At the low speeds involved an indication of stall cell frequency could be ascertained by observation of the static pressure manometer fluctuations.

A.R.C. C.P. No.620 May 1962

Shaw, R. and Lewkowicz, A.

THE CONSTRUCTION AND TESTING OF A LARGE AXIAL FLOW COMPRESSOR

The construction of a large low speed research compressor is described, together with some preliminary performance tests of a single stage arrangement at various speeds. The stalled region was investigated at all speeds, but at one speed a fuller investigation under stalled condition was carried out. At the low speeds involved an indication of stall cell frequency could be ascertained by observation of the static pressure manometer fluctuations.

A.R.C. C.P. No.620 May 1962

Shaw, R. and Lewkowicz, A.

THE CONSTRUCTION AND TESTING OF A LARGE AXIAL FLOW COMPRESSOR

The construction of a large low speed research compressor is described, together with some preliminary performance tests of a single stage arrangement at various speeds. The stalled region was investigated at all speeds, but at one speed a fuller investigation under stalled condition was carried out. At the low speeds involved an indication of stall cell frequency could be ascertained by observation of the static pressure manometer fluctuations.

Printed and published by
HER MAJESTY'S STATIONERY OFFICE

To be purchased from
York House, Kingsway, London, W.C.2
423 Oxford Street, London W.1
13A Castle Street, Edinburgh 2
109 St. Mary Street, Cardiff
39 King Street, Manchester 2
50 Fairfax Street, Bristol 1
35 Smallbrook, Ringway, Birmingham 5
80 Chichester Street, Belfast 1
or through any bookseller

Printed in England

S.O. Code No. 23-9013-20